Celestial Mechanics and Dynamical Astronomy manuscript No.
(will be inserted by the editor)

Dealing with Uncertainties in Angles-Only Initial Orbit Determination

Roberto Armellin · Pierluigi Di Lizia · Renato Zanetti

Received: date / Accepted: date

Abstract A method to deal with uncertainties in initial orbit determination (IOD) is presented. This is based on the use of Taylor differential algebra (DA) to nonlinearly map the observation uncertainties from the observation space to the state space. When a minimum set of observations is available, DA is used to expand the solution of the IOD problem in Taylor series with respect to measurement errors. When more observations are available, high order inversion tools are exploited to obtain full state pseudo-observations at a common epoch. The mean and covariance of these pseudo-observations are nonlinearly computed by evaluating the expectation of high order Taylor polynomials. Finally, a linear scheme is employed to update the current knowledge of the orbit. Angles-only observations are considered and simplified Keplerian dynamics adopted to ease the explanation. Three test cases of orbit determination of artificial satellites in different orbital regimes are presented to discuss the feature and performances of the proposed methodology.

1 Introduction

Orbit determination is typically divided into two phases. When the number of observation is equal to the number of unknowns, a nonlinear system of equations need to be solved. This problem is known as initial (or preliminary) orbit determination (IOD). When more observations are available, accurate

Roberto Armellin
IEF Marie Sklodowska-Curie Fellow, Departamento de Matemáticas y Computación, Universidad de La Rioja, 26006 Logrono, Spain (roberto.armellin@unirioja.es)
Pierluigi Di Lizia
Assistant Professor, Department of Aerospace Science and Technology, Politecnico di Milano, 20156 Milan, Italy (pierluigi.dilizia@esa.int)
Renato Zanetti
GN&C Engineer at NASA Johnson Space Center, 2101 NASA Road 1, Houston, Texas, 77058, United States (renato.zanetti@nasa.gov)

orbit determination can be performed. IOD typically delivers a single solution (or a limited number of solutions) that exactly produces the available observations. In addition, in IOD simplified dynamical models are often used (e.g. Keplerian motion) and measurement errors are not taken into account (the problem is deterministic). When more observations are available the approach becomes stochastic, because the additional observations include noise. This problem is usually set as an optimization one, in which the (optimal) solution is the one that minimizes the observation residuals. The solution is obtained via batch estimation, e.g. weighted nonlinear least squares, or a sequential estimation, e.g. extended Kalman Filtering.[1]

In this paper we focus our attention on the orbit determination of resident space objects (RSO) observed on a single passage with optical sensors. Thus, the problem is the one of an angles-only orbit determination. In order to determine, the orbit an IOD problem is solved followed by a procedure to update the initial solution based on the additional observations.

Angles-only IOD is an old problem. Gauss'[2] and Laplace's[3] methods are commonly used to determine a Keplerian orbit that fits with three astrometric observations. These methods have been revisited and analyzed by a large number of authors (e.g. 4–6) and new ones introduced more recently. The Double r-iteration technique of Escobal[7] and the approach of Gooding[8] are two examples of angles-only methods introduced for the IOD of RSO.

In 2012 Armellin at al.[9] proposed a IOD solver based on the solution of a Lambert's problem (between the second and the third observations) and a Kepler's problem (between the first and second observation). The method iterates on the slant ranges at the second and third observations in order to drive to zero the observational defects at the first observation. The iterations were carried out with a high-order extension of Newton's method enabled by differential algebra (DA). In addition, high order Taylor expansions were exploited to nonlinearly map the uncertainties from the observation space to the state space.

In this work a modified version of the method is proposed, in which all the three slant ranges are the problem unknowns. The approach is based on the solution of two Lambert's problems and using the continuity of the velocity vector at the central observation as constraint. The method has no restrictions on the geometry of the observations and it can deal with both short and long gaps. As in the previous work, the solution is obtained with a high-order Newton's iteration scheme enabled by DA. This approach allows the algorithm to both converge in few iterations and map uncertainties form the observation space to the state space. Thus, the initial orbit is already provided with statistical information.

When multiple observations on the same passage are available the IOD solution is updated. Instead of adopting a classical least squares approach (which employs the linearization of the dynamics and of the measurement functions[10]) high order inversion tools available in DA are exploited to nonlinearly map group of observations to the state space at a common epoch, thus producing full state pseudo-observations. The mean and covariance of these

pseudo-observations are nonlinearly computed by evaluating the expectation of the related high order Taylor polynomials. Finally, a linear updating scheme is utilized to update the current knowledge of the state mean and covariance.

The paper is organized as follows. A brief introduction on the DA tools used for the implementation of the algorithm is given first. This covers the methods to expand the solution of ordinary differential equations (ODE), compute the expansion of the solution of parametric implicit equations, and the algorithm to map statistics through nonlinear transformations. The following sections describe the main algorithms developed in this work, i.e. the angles-only IOD solver and the updating scheme. Simulated observational scenarios for a Geosynchronous Transfer Orbit (GTO), a Geosynchronous Orbit (GEO) and a Molniya are used to assess the performances of the implemented methods. Some final remarks conclude the paper.

2 Differential Algebra tools

DA supplies the tools to compute the derivatives of functions within a computer environment.[11] More specifically, by substituting the classical implementation of real algebra with the implementation of a new algebra of Taylor polynomials, any function f of v variables is expanded into its Taylor polynomial up to an arbitrary order n with limited computational effort. In addition to basic algebraic operations, operations for differentiation and integration can be easily introduced in the algebra, thusly finalizing the definition of the differential algebra structure of DA.[12,13] Similarly to algorithms for floating point arithmetic, also in DA various algorithms were introduced, including methods to perform composition of functions, to invert them, to solve nonlinear systems explicitly, and to treat common elementary functions.[14] The differential algebra used for the computations in this work was implemented in the software COSY INFINITY.[15] The reader may refer to Di Lizia et al.[16] for the DA notation adopted throughout the paper.

2.1 High-order expansion of the solution of ODE

An important application of DA is the automatic high order expansion of the solution of an ODE in terms of the initial conditions.[14,16] This can be achieved by replacing the operations in a classical numerical integration scheme, including evaluation of the right hand side, by the corresponding DA operations. This way, starting from the DA representation of an initial condition x_0, DA ODE integration allows the propagation of the Taylor expansion of the flow in x_0 forward in time, up to any final time t_f. Any explicit ODE integration scheme can be rewritten as a DA integration scheme in a straight-forward way. For the numerical integrations presented in this paper, a DA version of a 7/8 Dormand-Prince (8-th order solution for propagation, 7-th order solution for step size control) Runge-Kutta scheme is used. The main advantage of the

DA-based approach is that there is no need to write and integrate variational equations in order to obtain high order expansions of the flow. It is therefore independent of the particular right hand side of the ODE and the method is quite efficient in terms of computational cost.

2.2 Expansion of the solution of parametric implicit equations

Well-established numerical techniques (e.g., Newton's method) exist, which can effectively identify the solution of a classical implicit equation

$$\boldsymbol{f}(\boldsymbol{x}) = 0 \tag{1}$$

with $\boldsymbol{f} : \Re^n \to \Re^n$. Suppose an explicit dependence on a vector of parameters $\boldsymbol{p}$ can be highlighted in the vector function $\boldsymbol{f}$, which leads to the parametric implicit equation

$$\boldsymbol{f}(\boldsymbol{x}, \boldsymbol{p}) = 0. \tag{2}$$

Suppose the above equation is to be solved, whose solution is represented by the function $\boldsymbol{x}(\boldsymbol{p})$ returning the value of $\boldsymbol{x}$ solving (2) for any value of $\boldsymbol{p}$. Thus, the dependence of the solution of the implicit equation on $\boldsymbol{p}$ is of interest. DA techniques can effectively handle the previous problem by identifying the function $\boldsymbol{x}(\boldsymbol{p})$ in terms of its Taylor expansion with respect to $\boldsymbol{p}$. This result is achieved by applying partial inversion techniques as detailed in 16.

The final result is

$$[\boldsymbol{x}] = \boldsymbol{x} + \mathcal{M}_{\boldsymbol{x}}(\delta\boldsymbol{p}), \tag{3}$$

which is the k-th order Taylor expansion of the solution of the implicit equation. For every value of $\delta\boldsymbol{p}$, the approximate solution of $\boldsymbol{f}(\boldsymbol{x}, \boldsymbol{p}) = 0$ can be easily computed by evaluating the Taylor polynomial (3). Apparently, the solution obtained by means of the polynomial map (3) is a Taylor approximation of the exact solution of Eq. (2). The accuracy of the approximation depends on both the order of the Taylor expansion and the displacement $\delta\boldsymbol{p}$ from the reference value of the parameter.

2.3 Nonlinear mapping of the estimate statistics

Consider a random variable $\boldsymbol{x} \in \Re^n$ with probability density function $p(\boldsymbol{x})$ and a second random variable $\boldsymbol{y} \in \Re^m$ related to $\boldsymbol{x}$ through the nonlinear transformation

$$\boldsymbol{y} = \boldsymbol{f}(\boldsymbol{x}). \tag{4}$$

The problem is to calculate a consistent estimate of the main cumulants of the transformed probability density function $p(\boldsymbol{y})$. Since $\boldsymbol{f}$ is a generic nonlinear function, this formulation includes a wide range of problems involving uncertainty propagation (uncertainty propagation through nonlinear dynamics, uncertainty propagation through nonlinear coordinate transformations, etc.).

The Taylor expansion of $\boldsymbol{y}$ with respect to deviations $\delta\boldsymbol{x}$ can be obtained automatically by initializing the independent variable as a DA variable and evaluating (4) in DA framework. For each component y_i of $\boldsymbol{y}$, this procedure delivers

$$[y_i] = f_i([\boldsymbol{x}]) = y_i + \mathcal{M}_{y_i}(\delta\boldsymbol{x}) = \sum_{p_1+\cdots+p_n\leq k} c_{i,p_1\ldots p_n} \cdot \delta x_1^{p_1} \cdots \delta x_n^{p_n}, \tag{5}$$

where in this expression y_i is the zeroth order term of the expansion map, and $c_{i,p_1\ldots p_n}$ are the Taylor coefficients of the resulting Taylor polynomial

$$c_{i,p_1\ldots p_n} = \frac{1}{p_1!\cdots p_n!} \cdot \frac{\partial^{p_1+\cdots+p_n} f_i}{\partial x_1^{p_1} \cdots \partial x_n^{p_n}}. \tag{6}$$

The evaluation of (5) for a selected value of $\delta\boldsymbol{x}$ supplies the k-th order Taylor approximation of y_i corresponding to the displaced independent variable. Of course, the accuracy of the expansion map is function of the expansion order and can be controlled by tuning it.

The Taylor series in the form (5) can be used to efficiently compute the propagated statistics.[17,18] The method consists in analytically describing the statistics of the solution by computing the l-th moment of the transformed pdf using a proper form of the l-th power of the solution map (5).

For a generic scalar random variable x with pdf $p(x)$ the first four moments can be written as

$$\begin{cases} \mu = E\{x\} \\ P = E\{(x-\mu)^2\} \\ \gamma = \dfrac{E\{(x-\mu)^3\}}{\sigma^3} \\ \kappa = \dfrac{E\{(x-\mu)^4\}}{\sigma^4} - 3, \end{cases} \tag{7}$$

where μ is the mean value, P is the covariance, σ is the standard deviation, γ and κ are the skewness and the kurtosis, respectively,[19] and the expectation value of x is defined as

$$E\{x\} = \int_{-\infty}^{+\infty} xp(x)dx. \tag{8}$$

The moments of the transformed pdf in (4) can be computed by applying the multivariate form of Eq. (7) to the Taylor expansion (5). The result for the first two moments becomes

$$\begin{cases} \mu_{y_i} = E\{[y_i]\} = \displaystyle\sum_{p_1+\cdots+p_n\leq k} c_{i,p_1\ldots p_n} E\{\delta x_1^{p_1} \cdots \delta x_n^{p_n}\} \\ \boldsymbol{P}_{y_i y_j} = E\{([y_i]-\mu_i)([y_j]-\mu_j)\} = \displaystyle\sum_{\substack{p_1+\cdots+p_n\leq k, \\ q_1+\cdots+q_n\leq k}} c_{i,p_1\ldots p_n} c_{j,q_1\ldots q_n} E\{\delta x_1^{p_1+q_1} \cdots \delta x_n^{p_n+q_n}\}, \end{cases} \tag{9}$$

where $c_{i,p_1\ldots p_n}$ are the Taylor coefficients of the Taylor polynomial describing the i-th component of $[\boldsymbol{y}]$. Note that in the covariance matrix formula the

coefficients $c_{i,p_1\dots p_n}$ and $c_{j,q_1\dots q_n}$ are updated to include the subtraction of the mean. The coefficients of the higher order moments are computed by implementing the required operations (e.g. $([y_i]-\mu_i)([y_j]-\mu_j)$ for the second order moment) on Taylor polynomials in the DA framework. The expectation values on the right side of Eq. (9) are function of $p(\boldsymbol{x})$. It follows that if the initial distribution is known, all of the moments of the transformed pdf $p(\boldsymbol{y})$ can be calculated. The number of monomials for which it is necessary to compute the expectation increases with the order of the Taylor expansion and, of course, with the order of the moment we want to compute. Note that, at this time, no hypothesis on the initial pdf has been made. Thus, the method can be applied independently of the considered variable distribution.

We now consider the case in which $\boldsymbol{x}$ is a Gaussian random variable (GRV), $\boldsymbol{x} \sim \mathcal{N}(\boldsymbol{\mu}, \boldsymbol{P})$, in which $\boldsymbol{\mu}$ is the mean vector and $\boldsymbol{P}$ the covariance matrix. An important property of Gaussian distributions is that the statistics of a GRV can be completely described by the first two moments. In case of zero mean, the expression for computing higher-order moments in terms of the covariance matrix is due to Isserlis.[20] In physics literature, Isserlis's formula is known as the Wick's formula.

Let s_1 to s_n be nonnegative integers, and $s = s_1 + s_2 + \cdots + s_n$. Then the Wick's formula suggests that

$$E\{x_1^{s_1} x_2^{s_2} \dots x_n^{s_n}\} = \begin{cases} 0, & \text{if } s \text{ is odd} \\ Haf(\boldsymbol{P}), & \text{if } s \text{ is even} \end{cases} \tag{10}$$

where $Haf(\boldsymbol{P})$ is the hafnian of $P = (\sigma_{ij})$, which is defined as

$$Haf(\boldsymbol{P}) = \sum_{p \in \prod_s} \prod_{i=1}^{\frac{s}{2}} \sigma_{p_{2i-1},p_{2i}}, \tag{11}$$

and $\prod_s$ is the set of all permutations p of $\{1, 2, \dots, s\}$ satisfying the property $p_1 < p_3 < p_5 < \dots < p_{s-1}$ and $p_1 < p_2,\ p_3 < p_4, \dots, p_{s-1} < p_s$.[21]

We observe that the expectation value terms of Eq. (9) can be computed using Eq. (10), and the resulting moments can be used to describe the transformed pdf.

3 DA-based angles-only IOD

In the classical angles-only IOD problem, three optical observations at epoch t_i, with $i = 1, \dots, 3$ are available. The observations consist in three couples of right ascension and declination angles, (α_i, δ_i). These observations provide us with three inertial light of sights $\hat{\boldsymbol{\rho}}_i$, i.e. the unit vectors pointing from the observer (on the Earth's surface) to the observed object.

Assume to have first guess values of the slant ranges ρ_i or equivalently for the orbit radii r_i (e.g. from the solution of Gauss' 8th degree polynomial). We present a high order iterative procedure with the following objectives: a) refine

the values of ρ_i assuming Keplerian dynamics, and b) express the functional dependence of the solution of the IOD problem with respect to observation uncertainties in terms of a high-order Taylor polynomials.

We start by initializing the observations as DA variables:

$$\begin{aligned}[\boldsymbol{\alpha}] &= \boldsymbol{\alpha} + \delta\boldsymbol{\alpha} \\ [\boldsymbol{\delta}] &= \boldsymbol{\delta} + \delta\boldsymbol{\delta},\end{aligned} \tag{12}$$

in which we have grouped the observations in two homogeneous vectors, $\boldsymbol{\alpha} = (\alpha_1, \alpha_2, \alpha_3)$ and $\boldsymbol{\delta} = (\delta_1, \delta_2, \delta_3)$, and $\delta\boldsymbol{\alpha}$ and $\delta\boldsymbol{\delta}$ accounts for measurement uncertainties. The line of sight vectors at t_1, t_2 and t_3 become

$$\begin{aligned}[\hat{\boldsymbol{\rho}}_1] &= \hat{\boldsymbol{\rho}}_1 + \mathcal{M}_{\hat{\boldsymbol{\rho}}_1}(\delta\alpha_1, \delta\delta_1) \\ [\hat{\boldsymbol{\rho}}_2] &= \hat{\boldsymbol{\rho}}_2 + \mathcal{M}_{\hat{\boldsymbol{\rho}}_2}(\delta\alpha_2, \delta\delta_2) \\ [\hat{\boldsymbol{\rho}}_3] &= \hat{\boldsymbol{\rho}}_3 + \mathcal{M}_{\hat{\boldsymbol{\rho}}_3}(\delta\alpha_3, \delta\delta_3),\end{aligned} \tag{13}$$

where $\mathcal{M}_{\hat{\boldsymbol{\rho}}_i}$ is an arbitrary order Taylor polynomial that describes the effect of an observation uncertainty on the line of sight.

Similarly, we initialize DA variables on the topocentric distances at t_1, t_2 and t_3

$$\begin{aligned}[\rho_1]^{1^-} &= \rho_1^{1^-} + \delta\rho_1 \\ [\rho_2]^{1^-} &= \rho_2^{1^-} + \delta\rho_2 \\ [\rho_3]^{1^-} &= \rho_3^{1^-} + \delta\rho_3,\end{aligned} \tag{14}$$

or in more compact form

$$[\boldsymbol{\rho}]^{1^-} = \boldsymbol{\rho}^{1^-} + \delta\boldsymbol{\rho}, \tag{15}$$

where the superscript 1^- indicates the first step of the iterative procedure, and $\rho_1^{1^-}$, $\rho_2^{1^-}$, and $\rho_3^{1^-}$ are the guess values for the slant ranges.

The spacecraft position vectors can be written (by summing the known observer's locations) as

$$\begin{aligned}[\boldsymbol{r}_1] &= \boldsymbol{r}_1 + \mathcal{M}_{\boldsymbol{r}_1}(\delta\alpha_1, \delta\delta_1, \delta\rho_1) \\ [\boldsymbol{r}_2] &= \boldsymbol{r}_2 + \mathcal{M}_{\boldsymbol{r}_2}(\delta\alpha_2, \delta\delta_2, \delta\rho_2) \\ [\boldsymbol{r}_3] &= \boldsymbol{r}_3 + \mathcal{M}_{\boldsymbol{r}_3}(\delta\alpha_3, \delta\delta_3, \delta\rho_3).\end{aligned} \tag{16}$$

A DA-based Lambert's problem[22] can be solved between $[\boldsymbol{r}_1]$ and $[\boldsymbol{r}_2]$, and between $[\boldsymbol{r}_2]$ and $[\boldsymbol{r}_3]$. Using the DA-implementation of Lambert's problem we obtain two polynomial approximations for the velocity vector at t_2

$$\begin{aligned}[\boldsymbol{v}_2^-] &= \boldsymbol{v}_2^- + \mathcal{M}_{\boldsymbol{v}_2^-}(\delta\alpha_1, \delta\delta_1, \delta\alpha_2, \delta\delta_2, \delta\rho_1, \delta\rho_2) \\ [\boldsymbol{v}_2^+] &= \boldsymbol{v}_2^+ + \mathcal{M}_{\boldsymbol{v}_2^+}(\delta\alpha_2, \delta\delta_2, \delta\alpha_3, \delta\delta_3, \delta\rho_2, \delta\rho_3)\end{aligned} \tag{17}$$

Note that the above expressions of the velocity vector are different for two reasons. First, the starting values of the slant ranges are not the solution of the IOD problem; secondly, they have different functional dependence on the observation angles. The goal is thus a) to find the values of the slant ranges such that the velocity vector is continuos at the midpoint, i.e., we want to

find the exact values of ρ_1, ρ_2, and ρ_3, and b) to approximate the spacecraft state at t_2 as a Taylor polynomial in the observation uncertainties. We start by defining the Taylor map of the defects

$$[\Delta\tilde{\boldsymbol{v}}_2] = [\boldsymbol{v}_2^+] - [\boldsymbol{v}_2^-] = \Delta\tilde{\boldsymbol{v}}_2 + \mathcal{M}_{\Delta\tilde{\boldsymbol{v}}_2}(\delta\boldsymbol{\alpha}, \delta\boldsymbol{\delta}, \delta\boldsymbol{\rho}). \tag{18}$$

Note that, for the exact values of ρ_1, ρ_2 and ρ_3, the constant part of maps (18), $\Delta\tilde{\boldsymbol{v}}_2$, would be zero. We now need to find the variations $\delta\boldsymbol{\rho}$ necessary to cancel out these constants and to express $\boldsymbol{r}_2$ and $\boldsymbol{v}_2$ as Taylor polynomials in $\delta\boldsymbol{\alpha}$ and $\delta\boldsymbol{\delta}$ only. The first step is to work with an origin preserving map

$$[\Delta\boldsymbol{v}_2] = [\Delta\tilde{\boldsymbol{v}}_2] - \Delta\tilde{\boldsymbol{v}}_2 = \mathcal{M}_{\Delta\boldsymbol{v}_2}(\delta\boldsymbol{\alpha}, \delta\boldsymbol{\delta}, \delta\boldsymbol{\rho}) \tag{19}$$

and to build an augmented Taylor polynomial by adding identities in observation deltas

$$\begin{bmatrix} \Delta\boldsymbol{v}_2 \\ \delta\boldsymbol{\alpha} \\ \delta\boldsymbol{\delta} \end{bmatrix} = \begin{bmatrix} \mathcal{M}_{\Delta\boldsymbol{v}_2} \\ \mathcal{I}_{\boldsymbol{\alpha}} \\ \mathcal{I}_{\boldsymbol{\delta}} \end{bmatrix} \begin{bmatrix} \delta\boldsymbol{\alpha} \\ \delta\boldsymbol{\delta} \\ \delta\boldsymbol{\rho} \end{bmatrix}. \tag{20}$$

This polynomial map can be inverted using ad-hoc algorithms implemented in COSY INFINITY, yielding

$$\begin{bmatrix} \delta\boldsymbol{\alpha} \\ \delta\boldsymbol{\delta} \\ \delta\boldsymbol{\rho} \end{bmatrix} = \begin{bmatrix} \mathcal{M}_{\Delta\boldsymbol{v}_2} \\ \mathcal{I}_{\boldsymbol{\alpha}} \\ \mathcal{I}_{\boldsymbol{\delta}} \end{bmatrix}^{-1} \begin{bmatrix} \Delta\boldsymbol{v}_2 \\ \delta\boldsymbol{\alpha} \\ \delta\boldsymbol{\delta} \end{bmatrix}. \tag{21}$$

Extracting the three last lines we obtain

$$\left[\delta\boldsymbol{\rho}\right] = \left[\mathcal{M}_{\boldsymbol{\rho}}\right] \begin{bmatrix} \Delta\boldsymbol{v}_2 \\ \delta\boldsymbol{\alpha} \\ \delta\boldsymbol{\delta} \end{bmatrix}. \tag{22}$$

We now evaluate the map (22) in $[\Delta\boldsymbol{v}_2] = -\Delta\tilde{\boldsymbol{v}}_2$, obtaining

$$[\boldsymbol{\rho}]^{1^+} = \boldsymbol{\rho}^{1^+} + \mathcal{M}_{\boldsymbol{\rho}}(\delta\boldsymbol{\alpha}, \delta\boldsymbol{\delta}) \tag{23}$$

where the subscript 1^+ indicates the Taylor polynomial of the corrections of the topocentric distances to be applied at the end of the first iteration. This last step is the high-order counterpart of classical Newton's method.

The second iteration starts with the Taylor polynomials of the topocentric distances given by

$$[\boldsymbol{\rho}]^{2^-} = [\boldsymbol{\rho}]^{1^-} + [\boldsymbol{\rho}]^{1^+} = \boldsymbol{\rho}^{2^-} + \mathcal{M}_{\boldsymbol{\rho}}(\delta\boldsymbol{\alpha}, \delta\boldsymbol{\delta}, \delta\boldsymbol{\rho}) \tag{24}$$

where now the explicit dependence on the entire set of observables appears. Thus, from the second iteration, the Taylor polynomials (16)–(17) depend on all $(\delta\boldsymbol{\alpha}, \delta\boldsymbol{\delta}, \delta\boldsymbol{\rho})$. The iterative procedure ends when the values of $\Delta\tilde{\boldsymbol{v}}_2$ are smaller than a prescribed tolerance. The Taylor polynomials of the topocentric distances at the last iteration k are

$$[\boldsymbol{\rho}] = [\boldsymbol{\rho}]^{k^-} + [\boldsymbol{\rho}]^{k^+} = \boldsymbol{\rho} + \mathcal{M}_{\boldsymbol{\rho}}(\delta\boldsymbol{\alpha}, \delta\boldsymbol{\delta}) \tag{25}$$

Using these expressions, the spacecraft position and velocity vectors at t_2 assume the form

$$\begin{aligned}[\boldsymbol{r}_2] &= \boldsymbol{r}_2 + \mathcal{M}_{\boldsymbol{r}_2}(\delta\boldsymbol{\alpha}, \delta\boldsymbol{\delta}) \\ [\boldsymbol{v}_2] &= \boldsymbol{v}_2 + \mathcal{M}_{\boldsymbol{v}_2}(\delta\boldsymbol{\alpha}, \delta\boldsymbol{\delta}).\end{aligned} \tag{26}$$

or more compactly

$$[\boldsymbol{x}_2] = \boldsymbol{x}_2 + \mathcal{M}_{\boldsymbol{x}_2}(\delta\boldsymbol{\alpha}, \delta\boldsymbol{\delta}), \tag{27}$$

where $\boldsymbol{x}_2 = (\boldsymbol{r}_2, \boldsymbol{v}_2)$.

As a result of the iterative procedure, $\boldsymbol{r}_2$ and $\boldsymbol{v}_2$ exactly satisfy (in the two-body model) the nominal observation set $(\boldsymbol{\alpha}, \boldsymbol{\delta})$. Furthermore, for any displaced value of the observables, the solution of the preliminary determination problem is computed by evaluating the polynomial (26) in the corresponding values of $(\delta\boldsymbol{\alpha}, \delta\boldsymbol{\delta})$. Map (27) is an arbitrary order Taylor polynomial in $\delta\boldsymbol{\alpha}$ and $\delta\boldsymbol{\delta}$, which maps the uncertainties from the observable space to the spacecraft state space. In particular, using the approach described in Section "Nonlinear mapping of the estimate statistics" we can compute the statistical moments of $\boldsymbol{x}$, given the statistics of the measurements.

4 DA-inversion IOD

When more than three optical observations are available, the solution (reference state and associated statistics) of the IOD problem needs to be updated to include the additional information. This is carried out through a high-order filtering technique based on nonlinear mapping of statistics and linear update scheme, in which only the pdf of the measurements is constrained to be Gaussian.

The optimal linear estimate of a state $\boldsymbol{x}$ based on a measurement $\boldsymbol{y}$ is given by

$$\hat{\boldsymbol{x}} = \boldsymbol{\mu}_{\boldsymbol{x}} + \boldsymbol{P}_{\boldsymbol{xy}}\boldsymbol{P}_{\boldsymbol{yy}}^{-1}(\tilde{\boldsymbol{y}} - \boldsymbol{\mu}_{\boldsymbol{y}}) \tag{28}$$

where $\boldsymbol{\mu}_{\boldsymbol{x}}$ is the state mean, $\boldsymbol{P}_{\boldsymbol{xy}}$ is the joint covariance of the state and the measurement, and $\boldsymbol{P}_{\boldsymbol{yy}}$ is the covariance of the measurement. For a general non-linear measurement with additive noise $\tilde{\boldsymbol{y}} = \boldsymbol{h}(\boldsymbol{x}) + \boldsymbol{\eta}$, calculating $\boldsymbol{\mu}_{\boldsymbol{y}}$ and the covariance matrices requires full knowledge of the distribution of the state. This requirement has two consequences: first it means that the state and its uncertainty need to be propagated forward to the measurement time, and second that statistics of the measurement need to be calculated through a nonlinear transformation of the current state. In this work we propose addressing this issue in a different way. The state is always estimated at a fixed epoch time, and the nonlinear map to transport it to any other epoch is calculated with the DA framework. Instead of working with $\boldsymbol{y}$ as a function of $\boldsymbol{x}$, a full pseudo-measurement of the state is generated from $\boldsymbol{y}$; the inverse of the non-linear map from the state to the measurement is readily available from COSY INFINITY. The advantage of this approach is that only the distribution of the measurement noise is assumed Gaussian while the distribution of the state is left unconstrained.

Consider a time span $[t_0, t_f]$ and let $\boldsymbol{x}_k$ be the state variable at some time $t_k \in [t_0, t_f]$. Consider also a set of N measurements $\tilde{\boldsymbol{y}}_i$ given at times $t_i \in [t_0, t_f]$ with $i = 1, \ldots, N$. Given the current estimate of the state $\hat{\boldsymbol{x}}_k^-$ and the related error statistics, we can always define the estimated state as a DA variable and compute the predicted measurement at t_i in the DA framework. The relation between state and measurement is a nonlinear map that accounts for the forward propagation of the initial condition and the measurement function. Under proper conditions this relation can be inverted to map the observation space at t_i into the state space at t_k. The main cumulants of the resulting map can be computed as described in the previous section, with the assumption that the statistics of the measurement errors is Gaussian. The computed mean and covariance are exploited to update the knowledge of $\boldsymbol{x}_k$ using a linear update scheme. This can be done for groups of measurements for which the dimension of measurement vector $\boldsymbol{y}_i$ is equal to the dimension of the state vector, and the map is invertible.

The resulting method can be made recursive and summarized as follows. From the IOD algorithm we start from an initial value of the state estimate and covariance, $\hat{\boldsymbol{x}}_k^- = \boldsymbol{\mu}_{\boldsymbol{x}_k}^-$ and $P_{\boldsymbol{x}_k\boldsymbol{x}_k}^-$ (in general $t_k = t_2$, the epoch of the central observation in the IOD problem.) Define the current estimate at time of interest t_k as a DA variable; i.e.,

$$[\boldsymbol{x}_k] = \hat{\boldsymbol{x}}_k^- + \delta\boldsymbol{x}_k. \tag{29}$$

and propagate it to time t_i when a measurement becomes available. The result assumes the form of the following high-order Taylor expansion map

$$[\boldsymbol{x}_i] = \hat{\boldsymbol{x}}_i + \mathcal{M}_{\boldsymbol{x}_i}(\delta\boldsymbol{x}_k). \tag{30}$$

Note that the constant part of this map, i.e. $\hat{\boldsymbol{x}}_i$, is not the predicted mean at time t_i due to the nonlinearities of the dynamics (the relation $\hat{\boldsymbol{x}}_i = \boldsymbol{\mu}_{\boldsymbol{x}_i}$ holds true only if the state transition matrix is used). Then, use the measurement equation to compute

$$[\boldsymbol{y}_i] = \boldsymbol{h}([\boldsymbol{x}_i]) = \hat{\boldsymbol{y}}_i + \mathcal{M}_{\boldsymbol{y}_i}(\delta\boldsymbol{x}_k), \tag{31}$$

where $\boldsymbol{h}$ represents the measurement function. Figure 1(a) can be used by the reader to better understand the meaning of Maps (30)–(31).

The next step consists in defining an origin preserving map

$$\delta\boldsymbol{y}_i = [\boldsymbol{y}_i] - \hat{\boldsymbol{y}}_i = \mathcal{M}_{\delta\boldsymbol{y}_i}(\delta\boldsymbol{x}_k). \tag{32}$$

This polynomial map can be inverted if two conditions are satisfied: the map must be square and all the measurements must be independent. If these requirements are satisfied, we can invert the polynomial map (32) using algorithms implemented in COSY INFINITY, obtaining

$$\delta\boldsymbol{x}_k = \mathcal{M}_{\delta\boldsymbol{x}_k}(\delta\boldsymbol{y}_i). \tag{33}$$

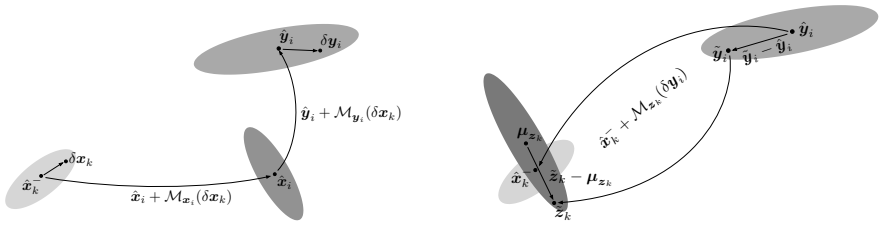

(a) Direct maps representation (b) Inverse map representation

Fig. 1: Sketch of the Taylor maps involved in the construction of the DA-base map inversion nonlinear filter.

We now replace $\delta\boldsymbol{x}_k$ in (29) with its expression from (33), yielding

$$[\boldsymbol{x}_k] = \hat{\boldsymbol{x}}_k^- + \mathcal{M}_{\boldsymbol{x}_k}(\delta\boldsymbol{y}_i). \tag{34}$$

This map now represents the pseudo-measurement of state $\boldsymbol{x}_k$ based on the observation $\tilde{\boldsymbol{y}}_i$, so it is renamed as

$$[\boldsymbol{z}_k] = \hat{\boldsymbol{x}}_k^- + \mathcal{M}_{\boldsymbol{z}_k}(\delta\boldsymbol{y}_i). \tag{35}$$

By construction the constant part of Eq. (35) is equal to the state estimate at step k, i.e. $\hat{\boldsymbol{x}}_k^-$, but its statistical moments are different to those of $\boldsymbol{x}_k$, due to the nonlinear contribution of $\mathcal{M}_{\boldsymbol{z}_k}(\delta\boldsymbol{y}_i)$ (as highlighted in Fig. 1(b)). We can now apply Eq. (9) to Taylor expansion (35) to compute the statistics of the random variable $\boldsymbol{z}_k$ and, in particular, the first two moments $\boldsymbol{\mu}_{\boldsymbol{z}_k}$ and $\boldsymbol{P}_{\boldsymbol{z}_k\boldsymbol{z}_k}$. The computed mean can be treated as the "predicted measure" of the state at time t_k, with measurement error defined by $\boldsymbol{P}_{\boldsymbol{z}_k\boldsymbol{z}_k}$. Thus, we can update the initial estimate and error covariance, using the least squares method. This can be done using the Kalman filter update equations that, applied to the current problem, read

$$\boldsymbol{K} = \boldsymbol{P}^-_{\boldsymbol{x}_k\boldsymbol{x}_k}\left(\boldsymbol{P}^-_{\boldsymbol{x}_k\boldsymbol{x}_k} + \boldsymbol{P}_{\boldsymbol{z}_k\boldsymbol{z}_k}\right)^{-1}, \tag{36}$$

$$\hat{\boldsymbol{x}}_k^+ = \hat{\boldsymbol{x}}_k^- + \boldsymbol{K}\left(\tilde{\boldsymbol{z}}_k - \boldsymbol{\mu}_{\boldsymbol{z}_k}\right), \tag{37}$$

$$\boldsymbol{P}^+_{\boldsymbol{x}_k\boldsymbol{x}_k} = (\boldsymbol{I} - \boldsymbol{K})\,\boldsymbol{P}^-_{\boldsymbol{x}_k\boldsymbol{x}_k}\,(\boldsymbol{I} - \boldsymbol{K})^T + \boldsymbol{K}\boldsymbol{P}_{\boldsymbol{z}_k\boldsymbol{z}_k}\boldsymbol{K}^T, \tag{38}$$

where $\hat{\boldsymbol{x}}_k^+$ is the updated estimate at time t_k and $\boldsymbol{P}^+_{\boldsymbol{x}_k\boldsymbol{x}_k}$ the related updated covariance matrix. When another measurement becomes available, we can define the state at time t_k as a new DA variable, centered in the new estimate $\hat{\boldsymbol{x}}_k^+$, and iterate the process. Note that $\tilde{\boldsymbol{z}}_k$ is the true state-measurement at t_i mapped to time t_k, which is readily available by evaluating Map (35) for $\delta\boldsymbol{y}_i = \tilde{\boldsymbol{y}}_i - \hat{\boldsymbol{y}}_i$.

We said that the polynomial map in Eq. (32) must be square in order to be invertible. It follows that if the measurement vector has smaller dimension than the state vector, after the first measurement is received we can not proceed

with the update, but we have to wait for additional measurements (i.e. in the optical case three observations are needed). When the number of scalar measurements equals the dimension of the state variable, we can define an augmented measurement vector that can be used to build Maps (31) and (32).

Once the final estimate of the state at time t_k is obtained, the statistics of the solution can be computed at any time via propagation and DA-based expectation evaluation.

5 Test Cases

The algorithms for IOD are run considering single-pass optical observations of three objects as listed in Table 1.

Table 1: Test cases: orbital parameters

Test Case		A	B	C
Orbit type		GEO	GTO	Molniya
SSC		26824	23238	40296
Epoch	JED	2457163.2824	2457167.1008	2457165.0708
a	km	42143.781	24628.972	26569.833
e	–	0.000226	0.699849	0.723221
i	deg	0.0356	3.962	62.794
Ω	deg	26.278	315.676	344.538
ω	deg	42.052	240.885	271.348
M	deg	72.455	13.735	347.726

The observations are all simulated from Teide Observatory, Tenerife, Canary Islands, Spain (observation code 954). The simulation windows are summarized in Table 2. For all the cases 15 equally spaced optical observations are simulated within the observation window. The spacecraft is considered observable when its elevation is above 10 deg, is in sunlight, and the Sun has an elevation lower than -7 deg. As a result, different observation gaps are considered, ranging from 522 s for the GTO case to 2160 s for the GEO case. The GTO object is observed before the apogee for an arc length of approximately 20.7 deg. The average separation between observations is 1.5 deg, with maximum and minimum values of 1.9 and 1.3 deg, respectively. The Molniya object is observed before the apogee on an arc length of 13.4 deg. In this case the mean, maximum, and minimum observation separations are 1, 1.1, and 0.8 deg. Finally, for the GEO case the observed arc has a length of 127.4 deg (with uniformly spaced observations).

For all the cases the central observations, i.e. observation ID 7, 8, and 9, are used for the IOD; thus, $\hat{\boldsymbol{x}}_8 = (\hat{\boldsymbol{r}}_8, \hat{\boldsymbol{v}}_8)$ and $P^-_{\boldsymbol{x}_8,\boldsymbol{x}_8}$ are the output of the IOD problem. The remaining observations are used for the update of $\hat{\boldsymbol{x}}_8$ and $P^-_{\boldsymbol{x}_8,\boldsymbol{x}_8}$.

Finally, pertaining to the accuracies, we consider Gaussian measurement noises with standard deviation of 0.5 arcsec.

Table 2: Test cases: observation windows

Test Case	Observation Window						Δt	$\sigma_{\alpha,\delta}$
	yr	mo	day_0	day_f	hr_0	hr_f	hr	arcsec
A	2015	MAY	22	23	21.000	05.400	0.600	0.5
B	2015	JUN	02	02	03.550	05.580	0.145	0.5
C	2015	MAY	22	22	20.600	23.400	0.200	0.5

All simulations are run on a MacBook Air with a 1.8 GHz Intel i5 CPU and 4 GB RAM.

5.1 DA-based angles-only IOD

The IOD algorithm is run 100 times for each of the three test cases described in Tables 1 and 2. The observation geometries are described in Figures 2(a), 2(c), and 2(e). For all the cases 6-th order computations are carried out. The DA-based IOD algorithm converges in all cases in, on average, three iterations (convergence is achieved when the euclidean norm of the velocity vector discontinuity at the central observation is less than 1×10^{-12} km/s). In all cases, the real solutions of the Gauss' 8th-degree polynomial are taken as first guesses for the unknown slant ranges.

The result of the DA-based IOD algorithm is the Taylor polynomial $[\boldsymbol{x}_8]$ (see Eq. (27)) that maps the observation uncertainties into uncertainties in the state space. This map is employed to compute the starting state estimate $\hat{\boldsymbol{x}}_8^-$ and covariance $P^-_{\boldsymbol{x}_8\boldsymbol{x}_8}$, evaluating the expectation of the monomials by assuming Gaussian statistics for measurement noise. Figures 2(b), 2(d), and 2(f) show the absolute value of the observation residuals associated to $\hat{\boldsymbol{x}}_8^-$ (normalized by the observations standard deviation) at the different observation epochs and for all the 100 simulations. As expected the residuals are minimal at the epochs of the IOD (i.e. ID 7, 8, and 9), whereas they steeply increase far from the central observations. In addition, note that $\hat{\boldsymbol{x}}_8^-$ does not exactly satisfy the IOD, as it is acually the constant part of the associated Taylor polynomial, $[\boldsymbol{x}_8]$, that does it (with an accuracy that depends on the threshold selected for algorithm convergence). The maximum differences between the constant part of the map and the computed mean are given in the first two columns of Table 3, where the contributions are split in position and velocity components. It is apparent that the nonlinearities play a minor role for the test case A, and this is confirmed by the fact that the residuals are minimal at observations 7, 8, and 9 for this test case (see Figure 2(b)).

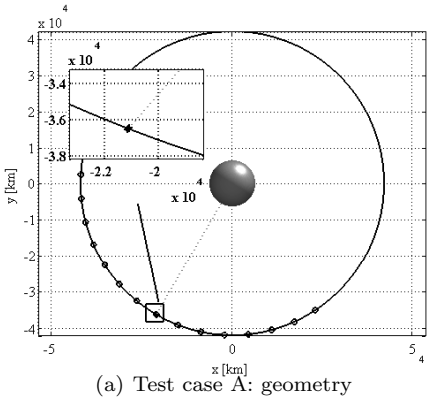

(a) Test case A: geometry

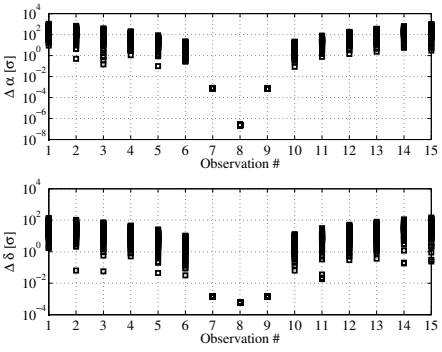

(b) Test case A: residuals

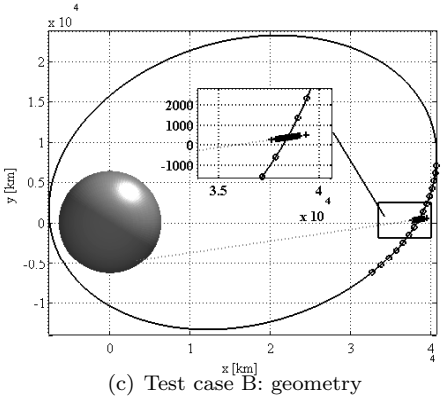

(c) Test case B: geometry

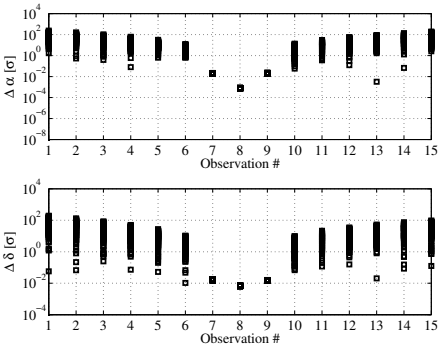

(d) Test case B: residuals

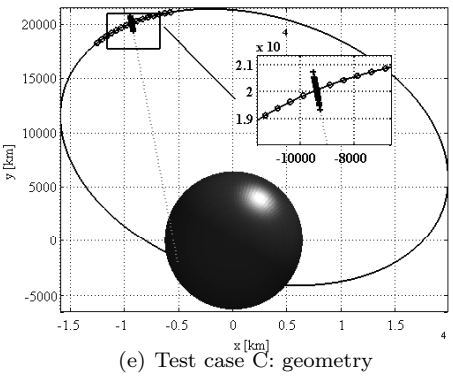

(e) Test case C: geometry

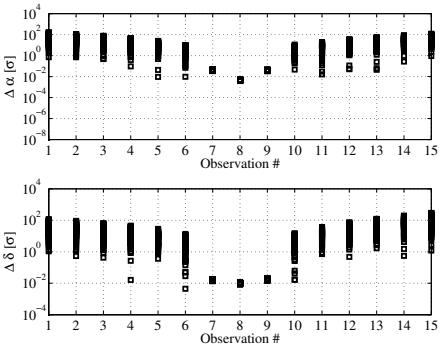

(f) Test case C: residuals

Fig. 2: Observation geometry and residuals

In all the cases the estimated covariance $P^-_{\boldsymbol{x}_8\boldsymbol{x}_8}$ is stretched along the line of sight directions as shown in the zoomed portions of Figures 2(a), 2(c), and 2(e). Higher nonlinearities affect test cases B and C, for which the uncertainty set is much more stretched. To quantify this, the maximum of the square root of the position and velocity covariance matrix eigenvalues (indicated with $\max \sigma_{\boldsymbol{r}_8}$ and $\max \sigma_{\boldsymbol{v}_8}$) are reported in Table 3.

Table 3: IOD: uncertainty set description.

Test Case	$\max \lvert\lvert \boldsymbol{r}_8 - \hat{\boldsymbol{r}}_8^- \rvert\rvert$ km	$\max \lvert\lvert \boldsymbol{v}_8 - \hat{\boldsymbol{v}}_8^- \rvert\rvert$ m/s	$\max \sigma_{\boldsymbol{r}_8}$ km	$\max \sigma_{\boldsymbol{v}_8}$ m/s
A	0.045	0.003	26.528	1.976
B	7.579	0.349	340.993	14.611
C	22.435	1.312	573.765	30.675

5.2 DA-based inversion IOD

The results obtained by applying the updating scheme presented in Sec. "DA-inversion IOD" are presented in this section. 100 simulations are run for each test case and all the computations are carried out at order 6, as for the DA-based IOD.

As we are considering 15 equally spaced optical observations, the maximum number of iterations (including the IOD using observations 7, 8, and 9) is 5. The updating scheme is stopped whenever the maximum number of iteration is reached or when the variation in the estimated state gets bigger than 5 times the maximum eigenvalues of the starting state covariance (this is considered as an anomaly in the updating scheme).

For all the cases a set of 4 plots is presented. In the first one the difference between the current state estimate and the true state (indicated as $||\hat{\boldsymbol{r}}_8 - \boldsymbol{r}_8^*||$ for position and $||\hat{\boldsymbol{v}}_8 - \boldsymbol{v}_8^*||$ for velocity) is plotted as function of the iteration number. Mean, maximum and minimum values for the considered 100 simulations are shown with different markers. In the second figure the maximum (over the 100 simulations) of the maximum position and velocity eigenvalues of the estimated covariance matrix are plotted as a function of the iteration number. Thus, the first two figures can be used to extract informations on state accuracy estimation and size of the estimated final uncertainty set. The third and fourth figures are about the observations residuals. More specifically, in the third figure the evolution of the mean residuals with the iteration number is highlighted using markers in gray scale (black markers for the last iteration); whereas in the fourth figure we plot the mean, maximum, and minimum values of the residuals (absolute value) at the the fifth iteration only.

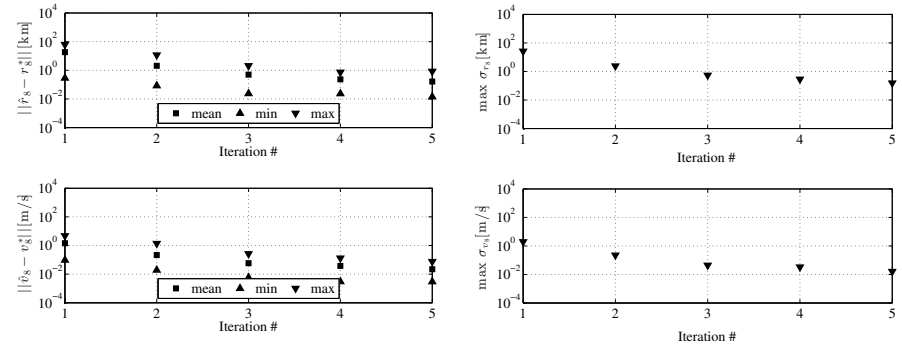

(a) Estimation error

(b) Estimated covariance size

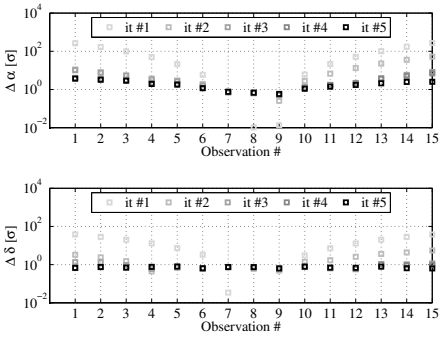

(c) Observation residuals convergence

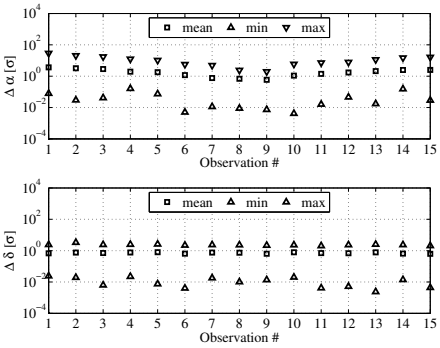

(d) Final observation residuals

Fig. 3: Test case A

Figures 3, 4, and 5 show all a similar behaviour of the relevant quantities. The accuracy of the estimation improves with iteration number, and the size of the estimated state covariance reduces accordingly. The observation residuals decrease and become more homogeneous with the iteration number. More accurate predictions are obtained for the Test Case A, thanks to both a longer observed arc and lower eccentricity of the orbit. In this case all the 100 simulations reach the 5-th iteration, with a mean final average estimation error of 0.164 km on position and 0.022 m/s on velocity. These errors increase to 3.353 km and 0.439 m/s for Test Case B, and to 8.520 km and 1.481 m/s for the Test Case C. Note that the 96% of the simulations reach the fifth iteration for the GTO case, and this number further reduces to 90% for the Molniya orbit.

Finally, in Figure 6 the results of 100 simulations using first order Taylor expansions are shown to highlight the effect of nonlinearities. It can be noticed that for the GEO case (Figure 6(a) and 6(b)) the updating algorithm is still convergent (although the average estimation error doubles with respect to 6-

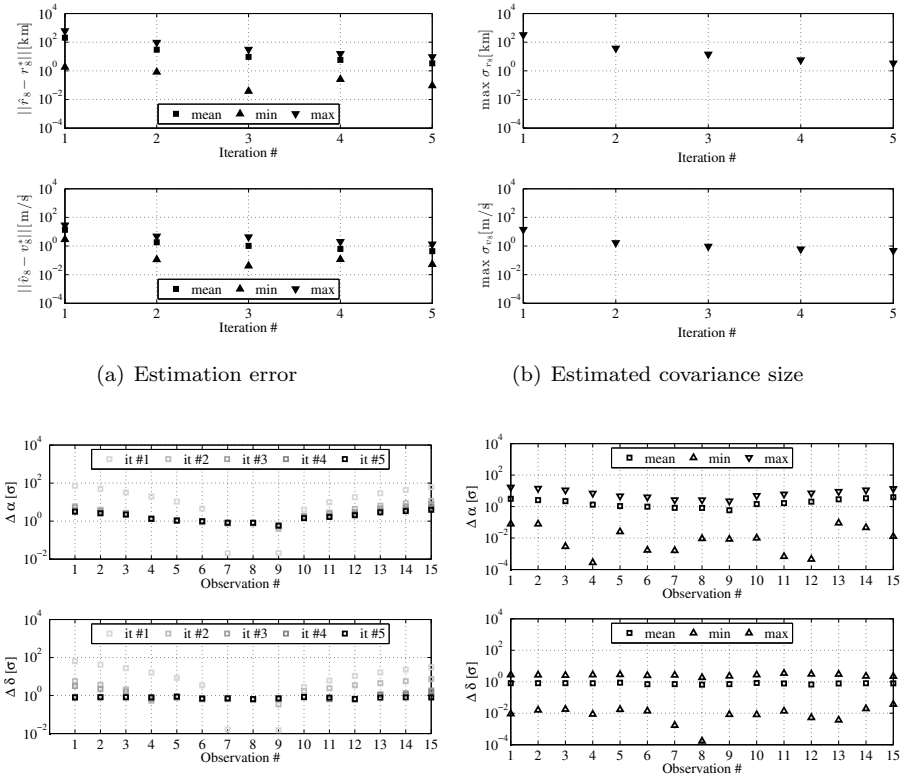

(a) Estimation error

(b) Estimated covariance size

(c) Observation residuals convergence

(d) Final observation residuals

Fig. 4: Test case B

order expansion) as both the estimation errors and the residuals decrease with the iteration number. This is not the case for both Test Case B and C, where the estimation errors and residuals decrease only up to the third iteration (i.e. when nine optical observations are used). Thus, in these cases a linear approximation is not sufficiently accurate in mapping, to the central epoch, the observations taken at the boundary of the visibility windows.

6 Conclusions

In this paper the problem of dealing with observation uncertainties in IOD is addressed. A fully nonlinear method for IOD is implemented based on the high order Taylor expansions delivered by DA computation. The method, based on the solution of two Lambert's problems, delivers the solution of IOD problem and nonlinearly maps uncertainties from the observations space to the state space already when the minimum (three) number of optical observations are

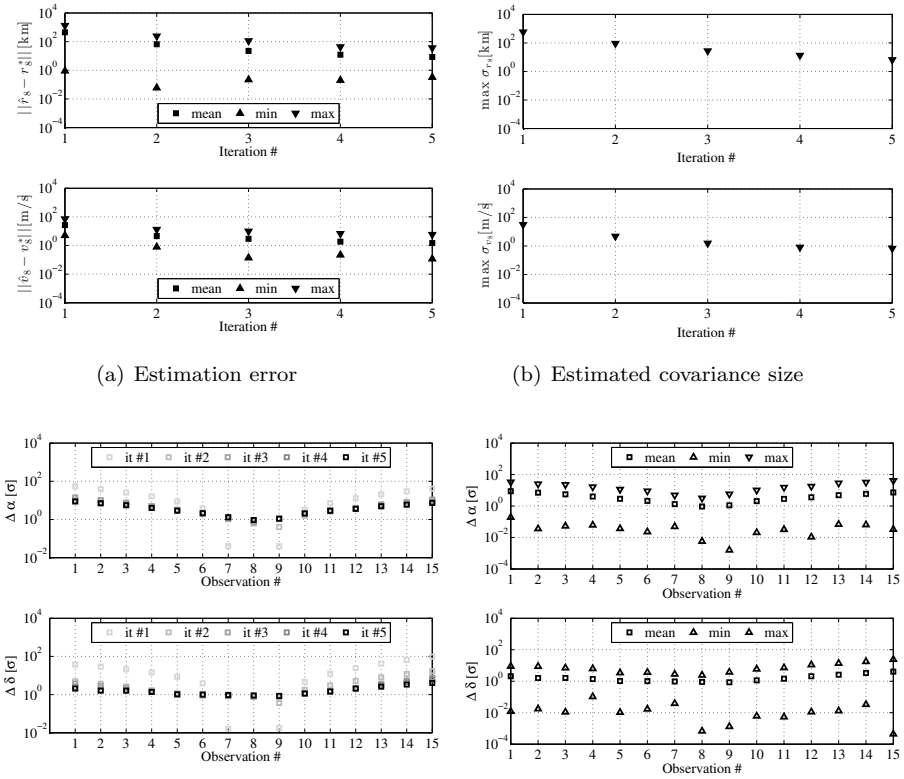

(a) Estimation error

(b) Estimated covariance size

(c) Observation residuals convergence

(d) Final observation residuals

Fig. 5: Test case C

considered. The algorithm converges for all the cases considered within, on average, three iterations. The average computational time is 3.6 s when 6-th order computations are carried out.

A linear scheme for updating the state's first two statistical moments is proposed when more optical observations are available in a single passage. This scheme is based on the generation of full state pseudo-observations at a common epoch, taking advantage of polynomial inversion tools available in DA. The required expectation are computed on high order Taylor polynomials, limiting the Gaussian assumption to the observation noises only. The updating scheme is shown to improve the accuracy of state estimation when short-dense observation arcs are available. The average computational time for the updating scheme is 1.91 s at order 6.

In the present work simplified keplerian dynamics are used. The algorithms can be easily extended to arbitrary dynamics by using the DA-based tools for the Taylor expansion of the solution of ODEs (see 17 for details) and by

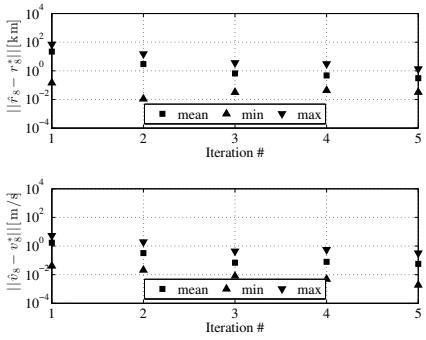

(a) Estimation error (Test Case A)

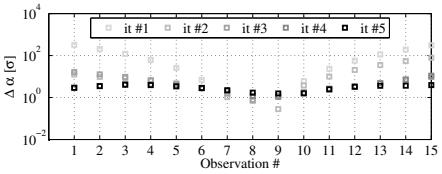

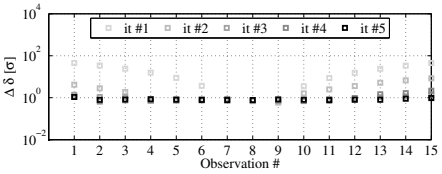

(b) Observation residuals convergence (Test Case A)

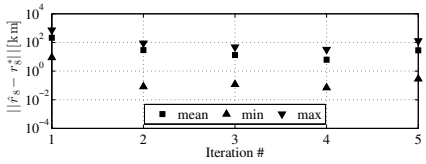

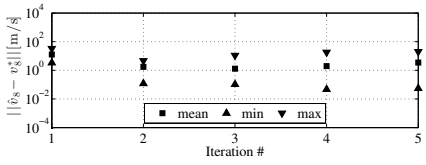

(c) Estimation error (Test Case B)

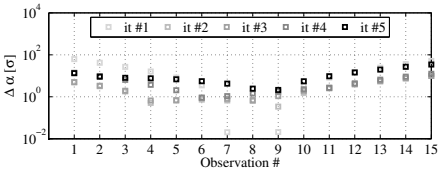

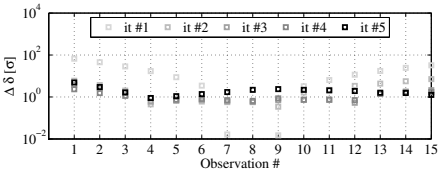

(d) Observation residuals convergence (Test Case B)

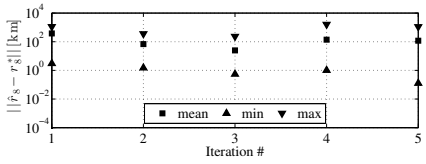

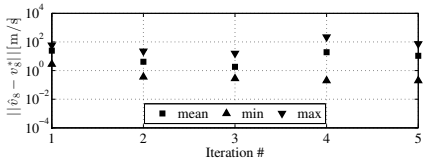

(e) Estimation error (Test Case C)

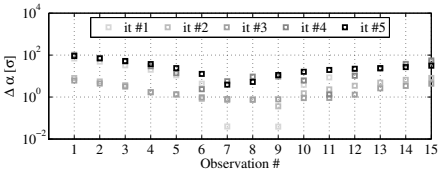

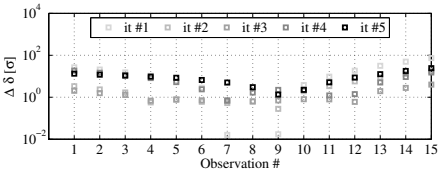

(f) Observation residuals convergence (Test Case C)

Fig. 6: Update results for 1st order computations

replacing the Lambert's solver with a DA-based algorithm for expanding the solution of two-point boundary values problems (as illustrated in 16). The authors plan to apply the algorithms to real observations including the case of short-dense radar observations.

Acknowledgements R. Armellin acknowledges the support received by the Sklodowska-Curie grant 627111 (HOPT - Merging Lie perturbation theory and Taylor Differential algebra to address space debris challenges).

References

1. D. A. Vallado and W. D. McClain, *Fundamentals of astrodynamics and applications*, Vol. 12. Springer Science & Business Media, 2001.
2. C. F. Gauss and C. H. Davis, *Theory of the Motion of the Heavenly Bodies Moving about the Sun in Conic Sections*. Courier Corporation, 2004.
3. P. Laplace, "Mémoires de l'Académie Royale des Sciences," *Paris, Reprinted in Laplace's Collected Works*, Vol. 10, 1780.
4. G. Merton, "A modification of Gauss's method for the determination of orbits," *Monthly Notices of the Royal Astronomical Society*, Vol. 85, 1925, p. 693.
5. A. Celletti and G. Pinzari, "Dependence on the observational time intervals and domain of convergence of orbital determination methods," *Periodic, Quasi-Periodic and Chaotic Motions in Celestial Mechanics: Theory and Applications*, pp. 327–344, Springer, 2006.
6. G. F. Gronchi, "Multiple solutions in preliminary orbit determination from three observations," *Celestial Mechanics and Dynamical Astronomy*, Vol. 103, No. 4, 2009, pp. 301–326.
7. P. R. Escobal, "Methods of orbit determination," *New York: Wiley, 1965*, Vol. 1, 1965.
8. R. Gooding, "A new procedure for the solution of the classical problem of minimal orbit determination from three lines of sight," *Celestial Mechanics and Dynamical Astronomy*, Vol. 66, No. 4, 1996, pp. 387–423.
9. R. Armellin, P. Di Lizia, and M. Lavagna, "High-order expansion of the solution of preliminary orbit determination problem," *Celestial Mechanics and Dynamical Astronomy*, Vol. 112, No. 3, 2012, pp. 331–352.
10. O. Montebruck and E. Gill, *Satellite Orbits*. New York: Springer-Verlag, 2nd ed., 2001.
11. M. Berz, *Differential Algebraic Techniques, Entry in Handbook of Accelerator Physics and Engineering*. New York: World Scientific, 1999a.
12. M. Berz, *The new method of TPSA algebra for the description of beam dynamics to high orders*. Los Alamos National Laboratory, 1986. Technical Report AT-6:ATN-86-16.
13. M. Berz, "The method of power series tracking for the mathematical description of beam dynamics," *Nuclear Instruments and Methods A258*, 1987.
14. M. Berz, *Modern Map Methods in Particle Beam Physics*. Academic Press, 1999b.
15. M. Berz and K. Makino, *COSY INFINITY version 9 reference manual*. Michigan State University, East Lansing, MI 48824, 2006. MSU Report MSUHEP060803.
16. P. Di Lizia, R. Armellin, and M. Lavagna, "Application of high order expansions of two-point boundary value problems to astrodynamics," *Celestial Mechanics and Dynamical Astronomy*, Vol. 102, No. 4, 2008, pp. 355–375.
17. M. Valli, R. Armellin, P. Di Lizia, and M. Lavagna, "Nonlinear mapping of uncertainties in celestial mechanics," *Journal of Guidance, Control, and Dynamics*, Vol. 36, No. 1, 2012, pp. 48–63.
18. R. Park and D. Scheeres, "Nonlinear Mapping of Gaussian Statistics: theory and Applications to Spacecraft trajectory Design," *Journal of Guidance, Control and Dynamics*, Vol. 29, No. 6, 2006.
19. G. Casella and R. Berger, *Statistical inference*. Duxbury Press, 2001.
20. L. Isserlis, "On a formula for the product-moment coefficient of any order of a normal frequency distribution in any number of variables," *Biometrika*, Vol. 12, No. 1 and 2, 1918.

21. R. Kan, "From moments of sum to moments of product," *Journal of Multivariate Analysis*, Vol. 99, No. 3, 2008.
22. R. Armellin, P. Di Lizia, F. Topputo, M. Lavagna, F. Bernelli-Zazzera, and M. Berz, "Gravity assist space pruning based on differential algebra," *Celestial mechanics and dynamical astronomy*, Vol. 106, No. 1, 2010, pp. 1–24.